ROS signaling by NOX4 drives fibroblast-to-myofibroblast transdifferentiation in the diseased prostatic stroma

Natalie Sampson[1], Christoph Zenzmaier[1], Lukas Bubendorf[2], Eugen Plas[3], Barbara Lener[1], Pidder Jansen-Dürr[1] & Peter Berger[1]*

[1] Institute of Biomedical Aging, Austrian Academy of Sciences, Innsbruck, Austria

[2] Institute of Pathology, University Hospital Basel, Basel, Switzerland

[3] Ludwig Boltzmann Institute for Andrology and Urology, Hospital Lainz, Vienna, Austria

Running Title: NOX4-derived ROS drives prostatic stromal transdifferentiation

Keywords:

aging, benign prostatic hyperplasia, insulin-like growth factor binding protein 3, prostate cancer, reactive oxygen species, selenium, transforming growth factor beta-1

*Corresponding author:

Tel +43 512 583919-24

Fax +43 512 583919-8

Email peter.berger@oeaw.ac.at

Non-standard abbreviations used:

BPH, benign prostatic hyperplasia; ct(BCS), charcoal-treated BCS; DPI, diphenylene iodonium; IGFBP3, Insulin-like growth factor binding protein 3; NOX, NADPH oxidase; qPCR, quantitative PCR; PCa, prostate cancer; PrSC, primary prostatic stromal cell; Se, selenium; Se-Cys, selenocysteine; SEPP1, Selenoprotein P plasma 1.

Abstract

Stromal remodeling via fibroblast-to-myofibroblast transdifferentiation promotes the development of benign prostatic hyperplasia (BPH) and prostate cancer (PCa). Elevated production of TGFbeta1 is considered to be the inducing stimulus. We demonstrate that NADPH oxidase 4 (NOX4)-derived ROS are essential signaling mediators of TGFbeta1-induced transdifferentiation in prostatic stromal cells. Induction of NOX4-derived ROS by TGFbeta1 coordinates the spatiotemporal activity of ERK1/2 and JNK, at least in part, via redox-dependent transcriptional regulation of DUSP phosphatases. ERK1/2 and JNK subsequently activate downstream transcriptional cascades leading to cytoskeletal remodeling and transdifferentiation. Consistently, *NOX4* expression correlated specifically with the myofibroblast phenotype *in vivo*. Thus, dysregulated NOX4-derived ROS signaling underlies the pathogenic activation of stromal fibroblasts in BPH and PCa.

Elevated NOX4-derived ROS signaling is supported by concomitant down-regulation of antioxidant enzymes and the selenium transporter Selenoprotein P plasma 1 (SEPP1). Moreover, loss of SEPP1 was observed in tumor-associated stroma of human PCa biopsies. Addition of selenium attenuated transdifferentiation by enhancing the expression of the ROS scavenging selenoenzymes TXN and TXNRD1, thereby depleting NOX4-derived ROS downstream of NOX4 induction. Collectively, this work indicates the potential clinical value of selenium and/or NOX4 inhibitors in preventing the functional pathogenic changes of stromal cells in BPH and PCa.

Introduction

Benign prostatic hyperplasia (BPH) and prostate cancer (PCa) are two of the most common diseases affecting elderly males (1). BPH is a classic age-associated progressive disease present in 20% of men at age 40 with progression to 70% at age 60 (2, 3). BPH is frequently associated with bothersome lower urinary tract symptoms (LUTS) with a lifetime risk for surgery of 25-30% (4, 5). PCa is the most common malignant tumor and second leading cause of male cancer death in Western societies. Whereas PCa is rare in men before their fifth decade, approximately 86% of PCa patients are over 65 years (6). Given their high prevalence, significant morbidity and age-associated incidence, current demographic trends underscore the socioeconomic and medical urgency for a better understanding of BPH and PCa etiology for disease prevention and improved therapeutic intervention.

Whilst distinct pathologies, BPH and PCa are both associated with changes in the stromal microenvironment that actively promote disease development (7, 8). The BPH and tumor-adjacent stroma (the latter also termed reactive stroma) are characterized by increased ECM deposition, capillary density and myofibroblasts, which arise from fibroblast transdifferentiation. In particular, elevated secretion of paracrine- and autocrine-acting mitogenic cytokines and growth factors by myofibroblasts promotes cellular proliferation, angiogenesis and tumorigenesis (9). Initial treatment for BPH and local-confined PCa exploits the androgen-dependence of the prostate by targeting local/systemic androgen metabolism and/or the androgen receptor itself resulting in apoptosis of androgen-dependent cells and thereby reduced prostate volume (10, 11). However, neither approach specifically addresses the stromal component of disease. Understanding the mechanisms underlying stromal remodeling in particular fibroblast-to-myofibroblast transdifferentiation may facilitate the development of preventative therapy or more effective treatment strategies.

TGFbeta1 (TGFβ1) is a multifunctional cytokine secreted in elevated concentrations by luminal epithelial cells in BPH (12) and by tumor cells in prostatic intraepithelial neoplasia (PIN), considered to be precursor tumorigenic lesions (13). Tissue and circulating TGFβ1 levels positively correlate with risk of BPH and PCa with particular alleles predisposing to

disease and more rapid tumor progression (14, 15). We and others previously demonstrated that TGFβ1 induces expression of ECM components and transdifferentiation of primary prostatic stromal fibroblasts (PrSCs) into myofibroblasts (16, 17). Moreover, exogenous administration of TGFβ1 is sufficient to induce myofibroblast differentiation and collagen production *in vivo* (18). Elevated production of TGFβ1 is thus likely a key inducer of pathogenic stromal reorganization. However, the molecular effectors through which TGFβ1 induces transdifferentiation and hence potential therapeutic targets remain unknown.

Various cellular stimuli (e.g. growth factors, cytokines such as TGFβ1, G protein-coupled receptor agonists and stress) induce regulated production of ROS. In such cellular contexts, ROS serve as second signaling messengers regulating diverse physiological processes, including proliferation, apoptosis, cytoskeletal remodeling, differentiation and migration (19). The downstream signaling effects of ROS are mediated via reversible oxidative modification of lipids, DNA and specific cysteine residues of certain proteins resulting in altered activity and function. Direct redox modification of transcription factors (NF-κB, AP1, HIF1, p53), protein kinases (MAPKs, PKB, PKC) and protein tyrosine phosphatases (PTPs) has been reported (20).

The NADPH oxidase (NOX) family is emerging as one of the most important sources of intracellular ROS. NOX enzymes are multisubunit transmembrane proteins that catalyze the reduction of oxygen using cytosolic NADPH as an electron donor generating superoxide, which may be subsequently dismutated to hydrogen peroxide (H_2O_2). In humans, seven NOX enzymes are currently known, NOX1-5 and DUOX1-2 as well as several activator “phox” subunits (21). Whilst NOX1 plays a role in host defense, ROS produced by other NOX enzymes act as second messenger molecules in signal transduction (21, 22). NOX4 has been implicated in the differentiation of cardiac fibroblasts associated with cardiac fibrosis and heart failure and lung mesenchymal cells associated with idiopathic lung pulmonary fibrosis (23, 24). However, the molecular mechanism(s) by which NOX4-derived ROS directed differentiation were not identified.

This work investigated the mechanisms driving fibroblast-to-myofibroblast transdifferentiation with the aim of identifying novel therapeutic targets to prevent stromal remodeling in BPH and PCa. We demonstrate that NOX4-derived ROS are essential signaling mediators of TGFβ1 that coordinate ERK1/2 and JNK spatiotemporal phosphorylation, which subsequently initiate downstream transcriptional programs of cytoskeletal remodeling and fibroblast-to-myofibroblast transdifferentiation. ROS signaling by NOX4 is positively supported by concomitant down-regulation of ROS scavenging enzymes, including several selenoproteins. Our data indicate the potential clinical value of selenium supplementation and/or NOX4 inhibitors in preventing the transformation of stromal cells in BPH and PCa.

Results

Dysregulation of redox-regulating enzymes during prostatic stromal fibroblast transdifferentiation

To investigate the molecular changes during BPH/PCa-associated fibroblast-to-myofibroblast transdifferentiation the expression profiles of TGFβ1-induced transdifferentiated and non-transdifferentiated PrSCs were analyzed by Affymetrix microarray. 1611 genes were identified with at least 2.5 fold change in their expression levels. Consistent with previous reports a significant proportion of regulated genes encoded ECM components or enzymes involved in ECM remodeling (9, 16) (Supplemental Table 1). One of the most strongly induced genes was *NOX4* (436.6 ± 20.8 fold). Of the other known NOX and associated genes, the regulatory phox subunit $p67^{phox}$ (*NCF2*) was also up-regulated (11.8 ± 4.7 fold). In addition, several genes encoding proteins with ROS scavenging function were significantly down-regulated, in particular Selenoprotein P plasma 1 (*SEPP1*, -7.2 ± 0.2 fold). These data were verified by quantitative PCR (qPCR; supplemental Figure 1). *NOX4* and *SEPP1* were 104.3 ± 8.0 and -14.2 ± 2.8 fold up- and down-regulated, respectively. The superior sensitivity of qPCR over microarray for the detection of low abundance transcripts revealed that despite their low basal expression *NOX1* and *NOX5* were marginally but significantly (p-value = 0.0005) down-regulated during TGFβ1-induced transdifferentiation (-2.8 ± 0.4 and -2.9 ± 0.4 fold, respectively). *NOX2* or *NOX3* were not detectably expressed in PrSCs (not shown). These data suggest that TGFβ1-induced transdifferentiation of PrSCs is associated with a NOX4-driven pro-oxidant shift in redox homeostasis.

Elevated ROS production precedes fibroblast transdifferentiation

To determine the functional significance of TGFβ1-induced *NOX4* expression, ROS production was measured in PrSCs. (Figure 1a). In comparison to basic FGF (bFGF) treated control cells, TGFβ1-transdifferentiated PrSCs produced significantly elevated ROS/H_2O_2 levels, which could be rapidly ablated with the flavoprotein and NOX inhibitor diphenylene iodonium (DPI). No significant change in ROS/H_2O_2 levels was observed upon PrSC

stimulation with PMA or ionomycin, which induce NOX1 and NOX5 activity, respectively (not shown). Thus, although their mRNAs are detectable, NOX1 and NOX5 proteins are present at functionally non-significant levels in PrSCs. Unlike other NOX enzymes, superoxide produced by NOX4 is barely detectable, possibly due to subcellular compartmentalization and/or rapid dismutation to H_2O_2 (25-27). Consistently, no significant induction of superoxide was detected by dihydroethidium-based assays upon PrSC stimulation with TGFβ1 compared to mock control cells (not shown). These data strongly suggest NOX4-derived H_2O_2 is the elevated ROS species during transdifferentiation in PrSCs.

Consistent with tetracycline-inducible NOX4 systems (25), elevated ROS production began 2-6 h after addition of TGFβ1. Peak levels were reached at 12 h and remained steady thereafter (Figure 1b). Cycloheximide completely abolished TGFβ1-mediated induction of ROS production indicating *de novo* protein synthesis is required (not shown). Elevated ROS production closely correlated with temporal induction of *NOX4* expression, whereas up-regulation of transdifferentiation markers *SMA (ACTG2*) and *Insulin-like growth factor binding protein 3* (*IGFBP3)* occurred later (12-24 h; Figure 1b), a finding confirmed at the protein level (Figure 4a). Thus, TGFβ1-dependent *NOX4* induction and elevated ROS production precede PrSC transdifferentiation.

Elevated ROS during transdifferentiation are specific non-stress inducing signaling molecules

When cellular ROS scavenging activity is deficient, high ROS levels may induce non-specific damage to DNA, proteins and lipids, termed oxidative stress (19). Oxidative stress-induced phosphorylation of p53 on Ser15 serves as an early indicator of DNA damage (28). Compared to positive control cells exposed to stress-inducing levels of H_2O_2, no detectable p53-Ser15 phosphorylation was observed in PrSCs incubated for 24-72 h with either bFGF or TGFβ1 (Figure 1c). Moreover, total protein carbonylation, an indicator of protein oxidation, did not significantly differ between bFGF and TGFβ1 treated PrSCs (not shown). In addition, only the reduced (active) form of the redox-sensitive nuclear phosphatase PTEN, which migrates slower under non-reducing SDS-PAGE relative to the oxidized (inactive)

phosphatase (29), was present in lysates of PrSCs stimulated for 24 h with bFGF or TGFβ1 (Figure 1d). Thus, despite sustained elevated ROS levels and reduced expression of ROS scavenging enzymes, ROS produced in response to TGFβ1 act as specific, non-stress inducing signaling molecules.

NOX4 is essential for fibroblast-to-myofibroblast transdifferentiation

To confirm that NOX4 is the ROS-producing source in response to TGFβ1, lentiviral-delivered shRNA was employed to knockdown (KD) NOX4. NOX4 shRNA dose-dependently reduced basal *NOX4* expression and significantly attenuated TGFβ1-induced *NOX4* expression (45.9 ±4.7 fold in vector and scrambled control cells) to just 8.3 ± 2.8 fold (MOI 2; Figure 2b). Similarly NOX4 shRNA reduced basal and TGFβ-stimulated NOX4 protein levels (Figure 2d). Moreover, TGFβ1-induced ROS production was reduced by 64.9% ± 9.1 (Figure 2c). Residual ROS levels were most likely due to incomplete silencing of NOX4 since higher levels of NOX4 lentivirus (MOI 5) further reduced TGFβ1-induced ROS production (not shown). However, cell viability was impaired at MOI >6, which is consistent with a threshold basal level of NOX4-derived ROS being essential for cell survival (30, 31). Subsequent experiments thus employed lentivirus at MOI 2. Under these conditions, NOX4 KD significantly attenuated TGFβ1-induction of transdifferentiation markers IGFBP3 and SMA at the mRNA (-3.7 ± 0.2 and -2.5 ± 0.4 fold, respectively; Figure 2b) and protein level (Figure 2d) compared to vector and scrambled control cells. Basal IGFBP3 and SMA mRNA and protein levels were not affected by NOX4 knockdown (Figure 2a and 2d, respectively). The morphological changes of PrSC fibroblast-to-myofibroblast transdifferentiation (16) were also inhibited upon NOX4 silencing (not shown). Thus, NOX4 is the predominant ROS-producing source induced by TGFβ1 in PrSCs and essential for fibroblast-to-myofibroblast transdifferentiation.

NOX4 coordinates cytokine-induced phosphorylation cascades

The intracellular response to cytokines including TGFβ1 is transduced by the concerted action of numerous kinases and phosphatases, whose activity is frequently sensitive to changes in redox homeostasis. We therefore examined the effect of NOX4 silencing on the phosphorylation status of different kinases during transdifferentiation. NOX4 KD reduced TGFβ1-stimulated but not basal phosphorylation of JNK and the TGFβ1 signaling intermediate SMAD2 indicating that their phosphorylation during transdifferentiation is at least in part NOX4-dependent. By contrast, both basal and TGFβ1-induced ERK1/2 phosphorylation was elevated upon NOX4 KD (2.1 ± 0.5 and 3.1 ± 0.3 fold, respectively; Figure 2d). Paradoxically, TGFβ1 induces pERK1/2 levels despite elevated NOX4. This suggests that ERK1/2 phosphorylation is regulated by the relative activity of NOX4-dependent and NOX4-independent mechanisms during PrSC transdifferentiation. TGFβ1-induced phosphorylation of PKC was not perturbed by NOX4 KD (not shown). p38 MAPK was not detectably phosphorylated in PrSCs either before or after transdifferentiation (not shown).

ERK1/2 and JNK kinases are required post-translationally for NOX4-derived ROS production

Kinase inhibitors were employed to evaluate the requirement of ERK1/2 and JNK kinases during transdifferentiation and compared to the effect of an ALK5/TGFβ receptor I (TGFβRI) inhibitor (SB413542). PKC inhibitors were also studied as PKC is implicated in regulating NOX isoforms at the transcriptional and post-translational level (32). Whilst an inhibitor of Ca^{2+}-dependent PKC isoforms (RO320432) had no significant effect on TGFβ1-induced ROS production or *NOX4* expression (Figure 3), a pan PKC inhibitor (RO318220) significantly reduced ROS production by 57% ± 5.9 (Figure 3a) and partially attenuated TGFβ1 induction of NOX4 mRNA (-3.0 fold ± 0.7; Figure 3b). However, transdifferentiation marker mRNA and protein levels were unchanged compared to cells treated with TGFβ1 alone (Figure 3b-c) most likely due to incomplete inhibition of NOX4 induction. Whereas these findings suggest that PKCs play no role in signaling downstream of NOX4, Ca^{2+}-independent PKC isoforms at least in part mediate TGFβ1-induced NOX4 transcriptional activation.

By contrast MEK/ERK inhibition (PD98059) attenuated TGFβ1 induction of the transdifferentiation marker IGFBP3 at both the mRNA and protein level but not that of SMA (Figure 3b-c). JNK inhibition (SP600125) attenuated TGFβ1-induction of IGFBP3 and SMA (Figure 3b-c) and morphological transdifferentiation (not shown). Thus, ERK1/2 and JNK are essential for coordinating the transdifferentiation response to TGFβ1. Although ERK1/2 and JNK inhibition did not alter TGFβ1-induction of NOX4 at the mRNA or protein level, ROS levels were significantly reduced by 45% ± 12.9 and 69% ± 13.3, respectively (Figure 3a-b and data not shown). Thus, whilst phosphorylation of ERK1/2 and JNK is regulated by *NOX4* induction (Figure 2d), their phosphoactivation apparently acts at the post-translational level in a feedback loop regulating NOX4-derived ROS production.

Negative feedback of NOX4-derived ROS via ERK1/2 phosphorylation

In time course assays of TGFβ1 stimulation, PKC and JNK phosphorylation occurred gradually (data not shown). By contrast, ERK1/2 underwent biphasic phosphorylation (Figure 4a-b) with the second sustained phase of activation temporally correlating with elevated ROS production (Figure 1b). Since redox-regulation of ERK1/2 has been reported, we investigated whether the kinetics (particularly the second phase) of ERK1/2 phosphorylation were disrupted upon NOX4 KD. As before, NOX4 KD potentiated the absolute amplitude of pERK1/2 levels but did not perturb the kinetics of ERK1/2 phosphorylation (Figure 4b).

Given that pharmacological inhibition of ERK1/2 (PD98059) appears to attenuate NOX4-mediated ROS production at a post-translational level (Figure 3), we next investigated whether late phase ERK1/2 phosphorylation may drive NOX4-dependent ROS production. Exposure of PrSCs to the MEK inhibitor PD98059 at a time point post TGFβ1 stimulation when late phase ERK1/2 phosphorylation has commenced (6 h) was sufficient to reduce TGFβ1-induced ROS production by 73.7% (± 5.6) and comparable to when the inhibitor was added prior to TGFβ1 stimulation (60.7% ± 2.6 at 0 h; Figure 4c). Thus, a complex feedback loop appears to exist in which NOX4-derived ROS coordinates the absolute level ERK1/2 phosphorylation, which in turn post-translationally regulates NOX4-derived ROS production.

NOX4 coordinates the expression of dual-specificity phosphatases during transdifferentiation

The catalytic activity of JNK and ERK1/2 is regulated by numerous phosphatases, in particular the MAPK phosphatase (MKPs) subset of dual specificity phosphatases (DUSPs), which display different tissue-specific expression, subcellular localization and MAPK substrate specificity (33, 34). Microarray data indicated that *DUSP2, -6* and *-10* are regulated 48 h after TGFβ1 stimulation, a finding confirmed by qPCR (24 h post TGFβ1 stimulation). TGFβ1 induced *DUSP2* expression (4.2 ± 0.8 fold) but down-regulated that of *DUSP6* and *DUPS10* (-4.3 ± 0.6 and -3.6 ± 0.3 fold, respectively, Figure 5a). NOX4 KD significantly attenuated these changes in DUSP gene expression (Figure 5a). In addition, basal expression of *DUSP6* (i.e. in non-transdifferentiated PrSCs) was elevated (2.5 ± 0.5 fold, p-value = 0.008) upon NOX4 KD. *DUSP1* and *PTP1B*, two other known redox-regulated phosphatases that dephosphorylate ERK1/2 and JNK, were neither regulated at the time points examined during transdifferentiation, nor altered upon NOX4 KD (Figure 5a and data not shown). Thus, NOX4 may determine the signaling response to TGFβ1 by coordinating the expression of selected MAPK phosphatases with distinct substrate specificity and subcellular localization.

NOX4 coordinates the subcellular localization of pERK

While DUSP10 targets pJNK, DUSP2 in the nucleus and DUSP6 in the cytoplasm dephosphorylate ERK1/2. The net effect of differential *DUSP2/6* regulation during transdifferentiation suggests that ERK1/2 is preferentially phosphorylated in the cytoplasm, a finding confirmed by immunuofluorescent staining and Western blotting of cytosolic extracts of PrSCs 24 h after TGFβ1 stimulation (Figure 5b and data not shown). Basal pERK (mock scrambled cells) was detectable in isolated PrSCs in a diffuse manner in the nucleus and cytoplasm (not shown). Upon NOX4 KD, basal pERK exhibited an identical localization however staining intensity was considerably higher and detectable in >95% of cells (not shown). This is consistent with higher levels of pERK by Western blotting (Figure 2d). In

scrambled control cells, TGFβ1 induced partial clearance of pERK from the nucleus and a significant induction in cytoplasmic pERK levels with strong perinuclear staining indicative of ER localization (Figure 5b). NOX4 KD attenuated the increase in cytosolic pERK, which remained evenly distributed within the nuclear and cytoplasmic compartments (Figure 5b). These findings are consistent with decreased expression of cytoplasmic DUSP6 and increased nuclear DUSP2 during TGFβ1-induced transdifferentiation and attenuation of these changes upon NOX4 silencing (Figure 5a). Collectively, these data indicate that transdifferentiation is associated with a NOX4-dependent restriction of pERK to the cytosol/ER.

NOX4 expression correlates with the myofibroblast phenotype in vivo

The data thus far implicate NOX4 in driving TGFβ1-mediated fibroblast-to-myofibroblast transdifferentiation. We therefore investigated whether NOX4 may play a role in the pathogenesis of BPH and PCa in which stromal remodeling and fibroblast transdifferentiation into myofibroblasts is characteristic. *NOX4* expression was verified by qPCR in non-tumor containing small prostate samples derived from radical prostatectomies (n = 13, Figure 6a) and compared to the expression of epithelial-, stromal- and myofibroblast-specific markers (Figure 6b). *NOX4* expression exhibited no correlation with 8 epithelial markers but weakly correlated with 6 stromal markers (R^2 = 0.21) and more strongly with 5 different myofibroblast markers (R^2 = 0.76). Thus, *NOX4* expression specifically correlates with the myofibroblast phenotype *in vivo*.

Loss of SEPP1 in tumor-associated stroma of human prostate biopsies

Selenium (Se) is an essential micronutrient that is incorporated as selenocysteine (Se-Cys) at the active site of selenoproteins, including SEPP1. Due to its high levels in plasma together with an unusually high Se-Cys content, SEPP1 is thought to predominantly function as a Se transport protein, however it may also possess intrinsic antioxidant properties (35, 36). *SEPP1* was significantly down-regulated during transdifferentiation (-14.2 ± 2.8 fold by

qPCR; supplemental Figure 1), a finding confirmed at the protein level (Figure 6c; -2.4 ± 0.2 fold).

To determine whether loss of SEPP1 is associated with pathogenic stromal remodeling *in vivo*, prostate biopsies from normal/BPH and PCa patients were stained for SEPP1 by immunohistochemistry (Figure 6d). Specificity of the SEPP1 signal was verified by pre-blocking with a peptide corresponding to residues 244-258 of human SEPP1 against which the antibody was raised (Figure 6d) (37). In normal/BPH prostate (n = 3), strong SEPP1 cytoplasmic staining was observed in basal and luminal epithelial cells and SMCs. Periglandular stromal cells (fibroblasts, perivascular and endothelial cells) were moderately stained (Figure 6d). However, in biopsies of PCa patients (Gleason 7, n = 3) SEPP1 immunoreactivity was specifically lost in the periglandular tumor-associated (reactive) stroma whereas adjacent bundles of smooth muscle and tumor cells stained positive (Figure 6d). Thus, consistent with the reduction of SEPP1 in transdifferentiated PrSCs (above), the remodeled prostatic stroma in PCa exhibits specific loss of stromal SEPP1.

Silencing of ROS signaling by selenium attenuates transdifferentiation

Se status regulates the expression and biosynthesis of selenoproteins (38, 39). Thus, reduced Se transport by SEPP1 may result in cellular Se deficiency, which subsequently decreases selenoenzyme synthesis and ROS scavenging activity, thereby potentiating NOX4-derived ROS signaling. To investigate whether exogenous Se was sufficient to restore antioxidant activity and inhibit transdifferentiation, PrSCs were exposed to subcytotoxic concentrations (5 nM) of selenium as inorganic sodium selenite. Selenite significantly attenuated TGFβ1-induced ROS production and expression of transdifferentiation markers without significantly altering their basal levels (Figure 7a-d). In addition, selenite elevated pERK1/2 and reduced pJNK/pSMAD2 levels as observed upon NOX4 KD (Figure 7d). TGFβ1-induced changes in *DUSP* expression were also attenuated by selenite (not shown). Consistently, selenite inhibited phenotypic switching associated with TGFβ1-induced transdifferentiation (Figure 7c). Moreover, selenite treatment 6 h after the addition of TGFβ1,

when ROS production has already commenced (Figure 1b) was sufficient to attenuate TGFβ1-induced transdifferentiation (not shown). Thus, selenite not only exerts a protective effect before ROS levels increase, but also mediates its inhibitory effects during active ROS production and once the transdifferentiation cascade has been initiated.

Selenite strongly reduced TGFβ1-induced ROS levels (9.0 ± 3.8 fold, p-value = 0.01) without significantly attenuating TGFβ1 induction of NOX4 mRNA (-2.1 ± 0.3 fold, p-value = 0.07) or protein (Figure 7a-d). This suggested that ROS scavenging activity was enhanced. Indeed, whilst selenite did not alter basal or TGFβ1-reduced *CAT* or *SEPP1* mRNA levels, basal expression of *SOD2, TXN* and *TXNRD1* was significantly induced by selenite (Figure 7e). Moreover, their down-regulation during TGFβ1-mediated transdifferentiation was completely reversed (Figure 7e). Collectively, these data indicate that selenite abrogates the initiated TGFβ1-induced transdifferentiation cascade by restoring antioxidant activity of specific ROS scavenging enzymes, which depletes NOX4-derived ROS thereby attenuating ROS signaling.

Discussion

Stromal remodeling via fibroblast-to-myofibroblast transdifferentiation promotes the development of BPH and PCa. Elevated production of TGFβ1, a potent inducer of fibroblast transdifferentiation *in vitro* and *in vivo*, is considered to be the inducing stimulus (12, 13, 16, 18). Several studies implicated NOX4 as a downstream TGFβ1 effector and mediator of transdifferentiation in mesenchymal cells of the heart and lung (23, 24, 40). However, the mechanism by which NOX4-derived ROS drive transdifferentiation remained to be elucidated. We demonstrate that ROS signaling by NOX4 induces fibroblast-to-myofibroblast transdifferentiation in PrSCs by modulating the spatiotemporal activity of MAPKs that coordinate downstream cytoskeletal remodeling and phenotypic transdifferentiation (summarized Figure 8). To our knowledge this is the first report demonstrating dysregulation of redox homeostasis in stromal remodeling in BPH and PCa.

NOX4 induction in PrSCs is an early event following TGFβ1-stimulation and mediated in part by Ca^{2+}-independent PKC isoforms. This is similar to vascular SMCs (41). However, PKC inhibitors incompletely attenuated *NOX4* induction implicating additional factors. The TGFβ-signaling intermediates SMAD2/3 and FOXH1 (which binds SMAD2) are likely candidates due to (i) their putative binding sites in the NOX4 promoter region (our observation, not shown), (ii) SMAD2/3 phosphorylation which occurs temporally upstream of TGFβ1-induced *NOX4* expression and (iii) the recent report that SMAD3 is required for *NOX4* induction by TGFβ1 in lung mesenchymal cells (24).

NOX4 is the major source of elevated ROS during PrSC transdifferentiation as demonstrated by isoform-specific KD. Moreover, ROS depletion by selenite attenuated transdifferentiation without significantly altering TGFβ1-induced NOX4 mRNA or protein levels. Thus, NOX4-derived ROS are critical mediators of transdifferentiation.

The signaling functions of ROS are primarily mediated by oxidative modification of redox-sensitive proteins. Generally, PTPs are inactivated whereas protein tyrosine kinases that activate MAPKs are activated by oxidation, thus promoting kinase cascades (20). PrSC transdifferentiation was associated with NOX4/ROS-dependent phosphorylation of JNK and

the C-terminal domain of SMAD2/3, the latter also reported in cardiac fibroblasts (23). TGFβ1 stimulation (and *NOX4* induction) also promoted ERK1/2 phosphorylation. Paradoxically however, NOX4/ROS depletion potentiated absolute levels of pERK1/2 but had no effect on the kinetics of biphasic ERK phosphorylation. Thus, pERK1/2 levels are positively and negatively regulated by the relative activity of ROS-independent and ROS-dependent mechanisms, respectively (Figure 8). Pharmacological inhibition confirmed the essential role of ERK1/2 and JNK in transducing the TGFβ1 transdifferentiation signal downstream of NOX4. Interestingly, the transdifferentiation cascade bifurcates at the level ERK1/2 and JNK, which are differentially required for IGFBP3 and SMA induction (Figure 8). This is consistent with reports that in models of pulmonary and dermal fibrosis TGFβ1 induction of collagen type I is ERK1/2-dependent, whereas fibronectin production is mediated via JNK (42, 43).

ROS exert their signaling effects not only at the post-translational level by oxidative modification of kinases and phosphatases, but also at the transcriptional level via redox-sensitive transcription factors, including NF-κB, AP1, HIF1, p53 (20). During transdifferentiation we observed NOX4/ROS-dependent transcriptional regulation of distinct MKPs (Figure 8). NOX4/ROS-dependent down-regulation of *DUSP10* would account for sustained ROS-dependent phosphorylation of JNK during transdifferentiation and reduced levels of pJNK upon NOX4 KD. Moreover, the reduction of nuclear and increase in cytoplasmic pERK1/2 levels during transdifferentiation is consistent with NOX4/ROS-driven elevated expression of *DUSP2* and down-regulation of *DUSP6*. The resulting pro-cytoplasmic shift in pERK1/2 during transdifferentiation is also consistent with reports that ERK1/2 phosphorylates cytoskeletal proteins (44) thereby accounting for its role in cytoskeletal remodeling during fibroblast-to-myofibroblast transdifferentiation.

Cytoplasmic pERK1/2 was visibly concentrated in perinuclear regions highly reminiscent of ER. This may reflect a mechanism similar to that observed in endothelial and COS7 cells in which ER-localized NOX4 oxidatively inactivated PTP1B, an ERK phosphatase localized on the cytoplasmic face of the ER (27). Efforts are underway to determine the localization of endogenous NOX4 and its oxidative targets in PrSCs.

Recent studies challenge the general consensus that NOX4 activity is primarily determined by its expression level with post-translational regulation by p38 MAPK and a newly identified protein (POLDIP2) being reported (45, 46). Pharmacological inhibition indicated that the ROS producing activity of NOX4 and/or activity of ROS scavenging enzymes in PrSCs is post-translationally regulated by ERK1/2 and JNK. An intriguing possibility currently being investigated is whether ERK/JNK directly phosphorylate NOX4 (supported by bioinformatics, not shown) or NOX4-associated proteins such as $p22^{phox}$ whose phosphorylation is known to regulate the activity of other NOX enzymes (47).

Whilst NOX4 regulates ERK1/2 and JNK phosphorylation, their activity is also required in a feedback manner for full activation of NOX-derived ROS production. This apparent feedback loop perhaps finely tunes the cellular response to differentiation/proliferation signals (Figure 8). Rapid transient ERK1/2 activation is associated with cell proliferation, whereas differentiation/cytoskeletal reorganization is mediated by sustained ERK1/2 phosphorylation (48). Our data indicate that this function of ERK1/2 may be due to its activation of NOX4-derived ROS, which subsequently activates downstream pathways leading to differentiation. Late phase ERK1/2 phosphoactivation may also serve as a counteracting survival pathway to overcome the apoptosis-inducing effects of sustained JNK activation (49).

In contrast to many peptide growth factors that induce transient ROS production, PrSCs undergoing transdifferentiation produced sustained elevated levels of ROS. This may be attributed to several sources, including (i) TGFβ1-autoactivation, (ii) integrin-induced NOX4-derived ROS that activates ECM remodeling MMPs (iii) pERK/pJNK-mediated activation of NOX4-derived ROS production and (iv) elevated deposition of ECM proteins that themselves stimulate NOX4 expression and ROS production (supplemental Table 1) (50-52). Thus, once initiated the remodeled stroma may sustain further ROS production in a positive feedforward mechanism leading to further fibroblast-to-myofibroblast transdifferentiation and consequently to stromal expansion, prostate enlargement (BPH) and in the presence of initiated epithelial cells to progression of PCa.

NOX4 specifically correlated *in vivo* with the myofibroblast phenotype, the predominant stromal cell type in BPH and PCa. Moreover, loss of SEPP1 was observed in the tumor-associated stroma of PCa biopsies. These findings together with the above *ex vivo* transdifferentiation data, strongly implicate a pro-oxidant imbalance in redox homeostasis in the pathogenic activation of myofibroblasts.

Whilst targeting NOX4 directly for therapeutic intervention of PCa/BPH remains a possibility, there are currently no specific NOX4 inhibitors. Although SEPP1 may possess intrinsic ROS scavenging activity, its primary function is considered to be the transport of Se (53). Thus, down-regulation of SEPP1, a direct transcriptionally suppressed target of TGFβ1/SMAD (54), may result in cellular Se deficiency. Given that Se status regulates the expression and biosynthesis of selenoproteins (38, 39), we hypothesized that SEPP1/Se deficiency may subsequently decrease selenoenzyme ROS scavenging activity and thereby potentiate NOX4-derived ROS signaling. Indeed, selenite abrogated transdifferentiation in a manner that precisely imitated NOX4 silencing.

Selenite reduced TGFβ-induced ROS without reducing *NOX4* mRNA levels, suggesting enhanced (selenoprotein) ROS scavenging activity. Supportively, selenite induced expression of the selenoenzymes *TXN* and *TXNRD1*. Selenite had no effect on *SEPP1* mRNA levels, most likely due to upstream direct inhibition by TGFβ1/SMAD (54). As a non-selenoprotein, selenite induction of *SOD2* was surprising but consistent with *in vitro* and *in vivo* findings of others (55-57). SOD2 induction may be required to ensure dismutation of superoxide, which combined with sufficient GPX activity to detoxify the resulting H_2O_2 into water perhaps serves to protect the mitochondria from excessive ROS. Collectively, these data demonstrate that selenite attenuates fibroblast-to-myofibroblast transdifferentiation most likely via enhanced biosynthesis of ROS scavenging selenoenzymes, which depletes TGFβ1-induced NOX4-derived ROS levels thereby preventing dysregulated NOX4/ROS signaling.

These findings are consistent with a large body of data in experimental animals that Se deficiency or supplementation increase or reduce tumor incidence, respectively (58-60).

However, several large-scale clinical and epidemiological studies yielded conflicting results relating plasma Se levels to the risk of PCa and the protective effect of Se supplementation on PCa incidence (61-64). Clearly, further well-designed studies are required to encompass a number of factors that may have contributed to these inconsistencies e.g. the source and dose of the Se supplement employed, baseline Se levels, individual Se requirements and genetic variations within antioxidant and selenoprotein genes (65, 66). However, the significant reduction in PCa incidence observed in the Nutritional Prevention of Cancer study suggests that Se supplementation may benefit subpopulations in whom activity of disease-relevant selenoenzymes are suboptimal, perhaps due to environmental and/or genetic factors (64, 65).

In summary, NOX4-derived ROS are essential TGFβ1 signaling effectors that define the spatiotemporal activity of ERK1/2 and JNK MAPKs via redox-specific regulation of *DUSP* phosphatase expression thereby activating downstream transcriptional cascades leading to fibroblast-to-myofibroblast transdifferentiation. ROS signaling is supported by the concomitant down-regulation of ROS scavenging (seleno)enzymes, which can be rescued by the addition of Se. These data demonstrate for the first time dysregulation of redox homeostasis in pathogenic activation of stromal fibroblasts in age-related proliferative diseases of the prostate and point to the potential clinical benefit of Se supplementation and/or local NOX4 inhibition in stromal-targeted therapy. Given that TGFβ signaling and myofibroblast activation are associated with numerous fibrotic disorders (e.g. idiopathic lung pulmonary fibrosis, nephrogenic systemic fibrosis, hypertrophic scarring, proliferative vitreoretinopathies, atherosclerotic lesions) and tumorigenesis, it will be interesting to see whether similar NOX4-dependent processes are at work.

Methods

Reagents

Reagents were from Sigma Aldrich unless otherwise specified. Human recombinant TGFβ1 was from R&D Systems, kinase inhibitors and concentrations employed were: TGFβ type 1 receptor activin receptor-like kinase ALK5 inhibitor SB431542 (1 μM, Tocris Bioscience), other kinase inhibitors were from Calbiochem: JNK (10 μM), SP600125; MEK, PD98059 (50 μM); PKC, RO320432 (Ca^{2+}-dependent) and RO318220 (pan) (1 μM). Antibodies were obtained as follows: p53, phospho-JNK and α-tubulin (Santa Cruz), IGFBP3 and phospho-SMAD2/3 (R&D Systems), β-actin, NOX4 and α-SMA (Sigma), phospho-p53, -PKC, -ERK1/2 and PTEN (Cell Signaling), SEPP1 was a kind gift from Holger Steinbrenner (Düsseldorf, Germany), HRP-conjugated secondary antibodies (Promega).

Primary cell culture

Human primary prostatic fibroblasts (PrSCs) were established from prostate organoids as described previously (16). PrSCs were maintained for routine culture in stromal cell growth medium (SCGM, Lonza) at 37°C in a humidified atmosphere of 5% CO_2. For all experiments cells of passage 2-4 were used directly from culture (not previously frozen). For transdifferentiation, PrSCs were incubated for 12 h in RPMI 1640 (Lonza) supplemented with 1% charcoal-treated BCS (ctBCS; Hyclone) and antibiotics. Cells were subsequently stimulated with either 1 ng/ml bFGF as mock control or 1 ng/ml TGFβ1 for the indicated duration. For kinase inhibition, cells were pretreated for 1 h with the appropriate kinase inhibitor or DMSO equivalent before stimulation with bFGF or TGFβ1 as indicated. All experiments were performed at least three times with primary cells from at least three different donors.

RNA isolation, cDNA synthesis and qPCR

Prostate samples from the ventral part of the prostate were obtained after radical prostatectomy (n = 13), snap frozen and stored in liquid nitrogen before homogenization and

total RNA isolation using TriZol reagent (Invitrogen). Total RNA from PrSCs was isolated using TriFast reagent (PeqLab). cDNA synthesis and qPCR were performed as described (16). Primer sequences are given in Supplementary Table 2. For PrSC experiments cDNA concentrations were normalized by the internal standard hydroxymethylbilane synthase (HMBS), a moderate copy number housekeeping gene not regulated under the experimental conditions employed. Relative changes in gene expression were calculated as described (67). For prostate samples cDNA concentrations were normalized to HMBS and EEF1A1. NOX4 expression was compared to the geometric mean expression (ct) value of epithelial markers (KLK3, KLK2, DPP4, EHF, CDH1, TMPRSS2, CORO2A and KRT5), stromal markers (SMA, IGF1, TGFB1I1, OGN, CNN1, PAGE4) or myofibroblast markers (COMP, PLN, RARRES1, COL4A1, TNC).

Microarrays

PrSCs from three independent donors incubated overnight in 1% ctBCS/RPMI were stimulated either with 1 ng/ml bFGF as mock control or with 1 ng/ml TGFβ1 for 48 h. 2 μg total RNA from each donor were pooled and hybridization to Affymetrix Human Genome U133 Plus 2.0 GeneChips® was performed at the Microarray Facility (Tübingen, Germany). A biological replicate array was performed. Raw expression data were normalized using the GRCMA algorithm at CARMAweb (68, 69). The complete microarray dataset is available at ArrayExpress (E-MEXP-2167).

Lentiviral-mediated knockdown of NOX4

NOX4, scrambled and empty vector shRNA lentiviral particles were generated as described (70). For viral transduction, PrSCs were seeded in appropriate vessels in SCGM. The following day, media was replenished supplemented with 8 μg/ml polybrene and virus-containing supernatant at the MOI indicated. After 96 h, cells were incubated overnight in 1% ctBCS supplemented RPMI containing antibiotics before stimulation with 1 ng/ml TGFβ1 for

the duration indicated. In all experiments, empty pLKO.1 vector and/or scramble shRNA vector (Addgene plasmid 1864) were used as controls.

ROS detection

ROS production was detected using a chemiluminescent protocol. Briefly, 20,000 PrSCs in triplicate in 24well plates were incubated overnight in 1% ctBCS in RPMI before stimulation as indicated. Cell monolayers were rinsed with pre-warmed Hanks' Buffered Salt Solution without Ca^{2+} and Mg^{2+} (HBSS, Lonza) and incubated with 4 U/ml horseradish peroxidase and 10 μg/ml luminol in HBSS. Luminescence was measured on a Chameleon luminescence counter (HVD Bioscience) at 37°C. Values were normalized against cell number using the Cell Titer Glo Luminescence assay reagent (Promega).

Western blotting and immunohistochemistry

Isolation of total cell lysates and Western blotting were performed as described (16) and normalized for total protein content via Bradford assay (Bio-Rad). For analysis of PTEN oxidation lysates were prepared in the presence of 10 mM N-ethylmaleimide (NEM) to prevent cysteine oxidation during lysis. Prostate tissue sections from paraffin blocks of formalin-fixed whole biopsy specimens (obtained from the archives of the Institute of Pathology at the University Hospital Basel (Switzerland)) were processed for immunohistochemistry as described (71). Where indicated SEPP1 antibody (1:500) was pre-blocked overnight at 4°C in 1% BSA/PBS containing 50μg/ml blocking peptide (244-258aa, Alta Bioscience, UK).

Preparation of membrane and cytosolic extracts for NOX4 detection

For NOX4 detection by Western blotting, PrSCs in 6 cm dishes were scraped into 100 μl PBS containing COMPLETE® protease inhibitor cocktail (Roche) and snap-frozen in liquid N_2. Upon thawing, samples were vortexed, sonicated briefly and centrifuged at 13,000 rpm for 15 min at 4°C. Supernatants (cytosolic extracts) were recovered and protein content

determined by Bradford assay (Bio-Rad Laboratories). Pellets were resuspended in 0.1 μl Membrane Extraction Buffer (20 mM MOPS, pH 7.2, 2% Triton X-100, 0.5 M NaCl and 0.25 M sucrose) per 1 μg total protein concentration of the corresponding cytosolic extract. The samples were sonicated, the clarified supernatant recovered as the membrane extract and protein content normalized by Bradford assay before analysis by Western blotting as above.

Immunofluorescence

PrSCs seeded on glass coverslips were infected with lentivirus as before before stimulation with 1 ng/ml TGFβ or mock control for 24 h. Cells were fixed, permeabilized and stained with anti-phospho ERK1/2 (Cell Signaling Technology) according to the manufacturer's instructions. Primary antibody was detected with AlexaFluor546 conjugated anti-rabbit antibody (Invitrogen). Nuclei were counterstained with SYTOX® (Invitrogen) before embedding in 90% glycerol. Confocal images were acquired using an UltraVIEW RS (Perkin Elmer) mounted on an Olympus IX-70 inverse microscope (Olympus) using a 40x water immersion objective. Constant laser intensity settings were used.

Statistical analysis

Numerical data are presented as mean ±SEM from at least three independent experiments using independent donors. Statistical evaluation was performed using a Student's *t*-test (ns, not significant; *, $p < 0.05$; **, $p < 0.01$).

Acknowledgements

The authors gratefully acknowledge Professor Stephan Dirnhofer (University Hospital Basel, Switzerland) for assistance with immunohistochemistry and Dr Martin Hermann (Tyrolean Cancer Research Institute, Innsbruck) for confocal imaging. This work was supported by the Austrian Science Fund (FWF; NRN S9307-B05 and S9305-B05), NS is the recipient of a Lise Meitner Scholarship (FWF; M903-B05). The authors have no competing financial interests.

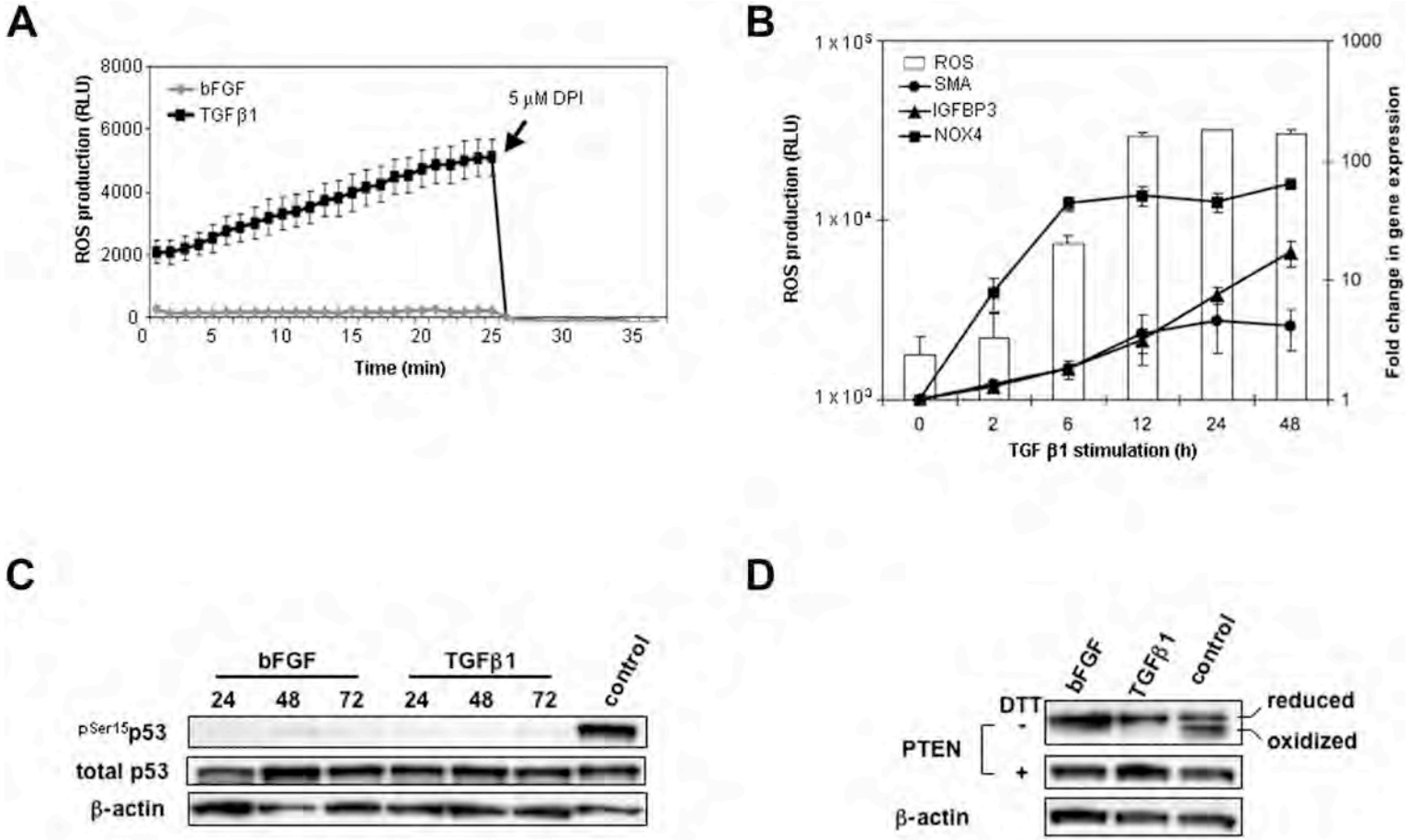

Figure 1

Sustained ROS production precedes fibroblast-to-myofibroblast transdifferentiation.

(A) ROS production was measured real-time in PrSCs 24 h post stimulation with TGFβ1 or bFGF as control. Where indicated 5 μM DPI was added and luminescence re-measured. Mean values of triplicate wells are shown (±SEM). A representative example of at least three experiments using independent donors is shown. (B) Time course assay of ROS production (left x-axis) and fold change in gene expression (right x-axis) in PrSCs stimulated for the indicated duration with TGFβ1. Mean values obtained from at least three experiments using independent donors are shown (± SEM). (C, D) Western blotting with the indicated antibodies of lysates from PrSCs stimulated with bFGF or TGFβ1 for the indicated duration (hours) (C) or 24 h (D). As positive control PrSCs incubated with bFGF for 24 h were treated with 75 μM H_2O_2 for 90 min. A representative blot from three independent donors is shown.

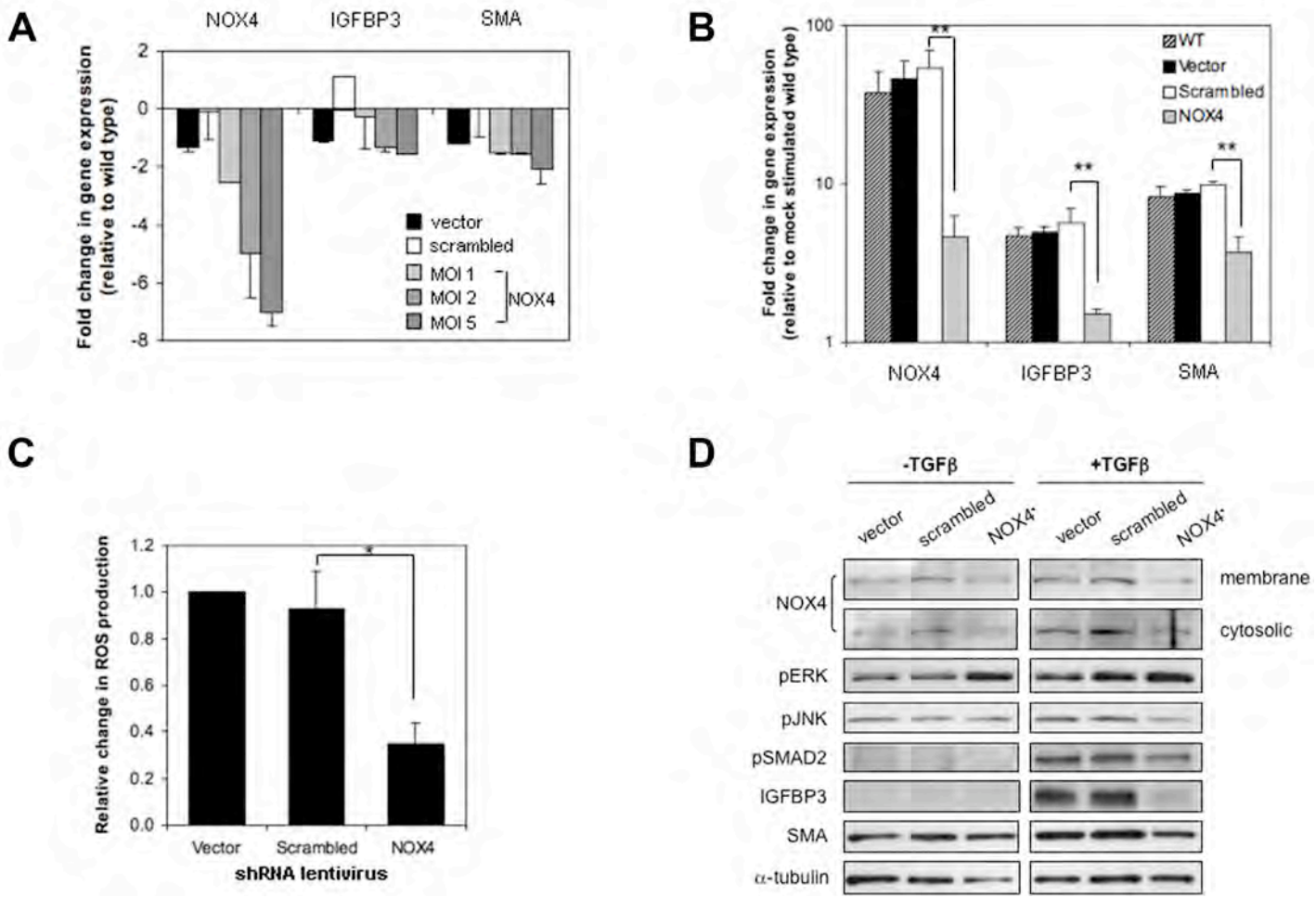

Figure 2

NOX4-derived ROS is essential for TGFβ1-mediated fibroblast-to-myofibroblast transdifferentiation.

(A, B) qPCR of *NOX4, IGFBP3* and *SMA* expression in PrSCs infected with the appropriate shRNA-expressing lentivirus at the indicated MOI (A) or MOI 2.0 and stimulated for 24 h with TGFβ1 (B). Mean values (± SEM) of at least three experiments using independent donors are shown relative to mock treated WT (non-transduced) PrSCs. (C) ROS production of PrSCs treated as in (B). Values represent mean fold change in ROS production (± SEM) from triplicate wells in at least three experiments using independent donors relative to vector control cells. (D) Western blotting of total cell lysates from PrSCs treated as in (C) in the presence or absence of TGFβ1 for 24 h. Detection of NOX4 was performed in parallel prepared membrane and cytosolic extracts. A representative example of four independent experiments using different donors is shown. Significance is indicated (* $p < 0.05$, ** $p < 0.01$).

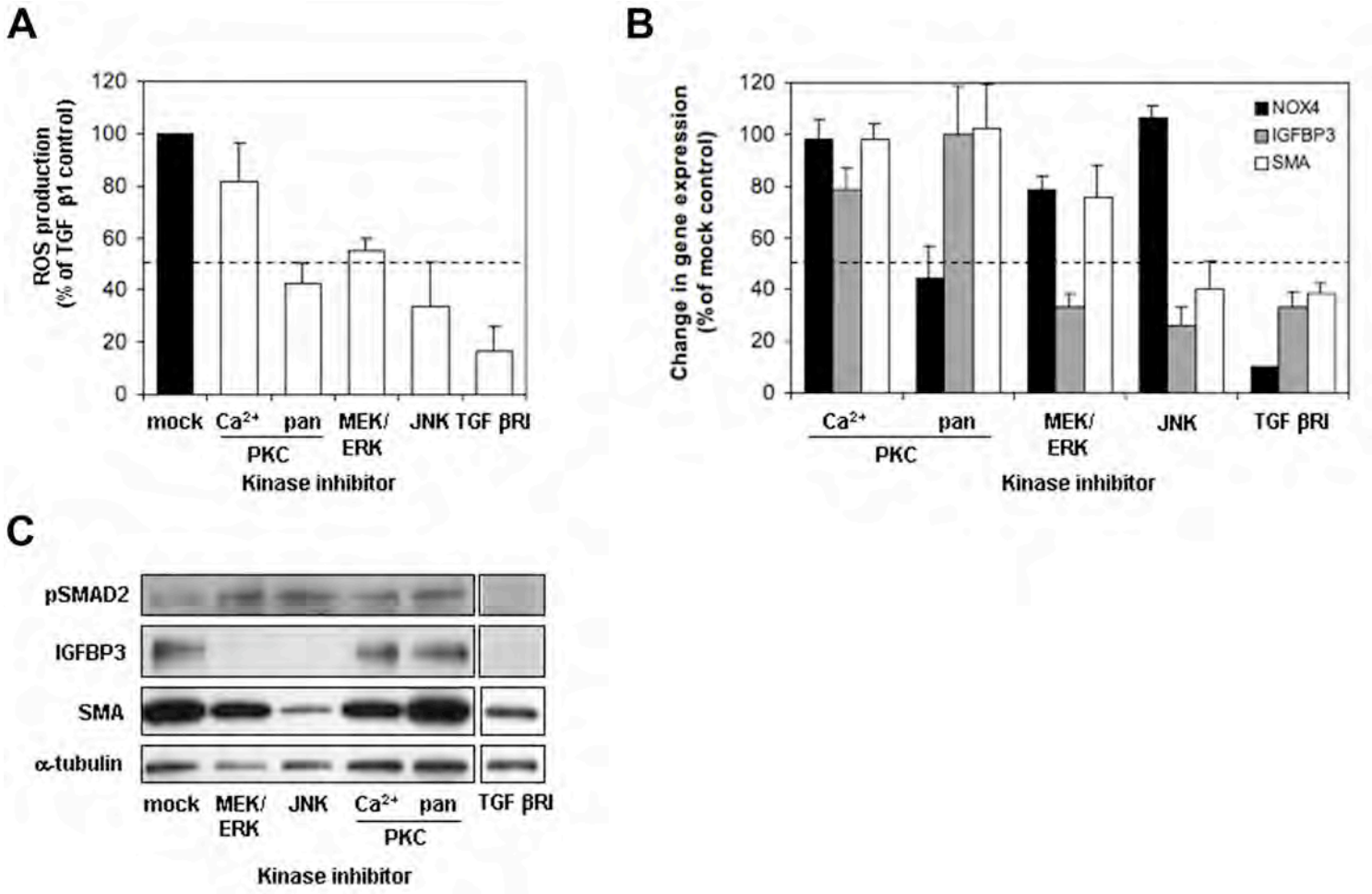

Figure 3

Post-translational ERK1/2- and JNK-dependent activation of TGFβ1-induced ROS production.

PrSCs were treated with TGFβ1 and the indicated kinase inhibitor as described in Methods for 24 h before determination of ROS levels (A), qPCR of the indicated genes (B) and Western blotting of total cell lysates (D) using the antibodies indicated. (A, B) Mean values from at least three independent experiments using different donors are shown expressed as percentage (± SEM) relative to mock control treated with TGFβ1 and DMSO equivalent. (C) A representative example of three independent experiments using different donors is shown.

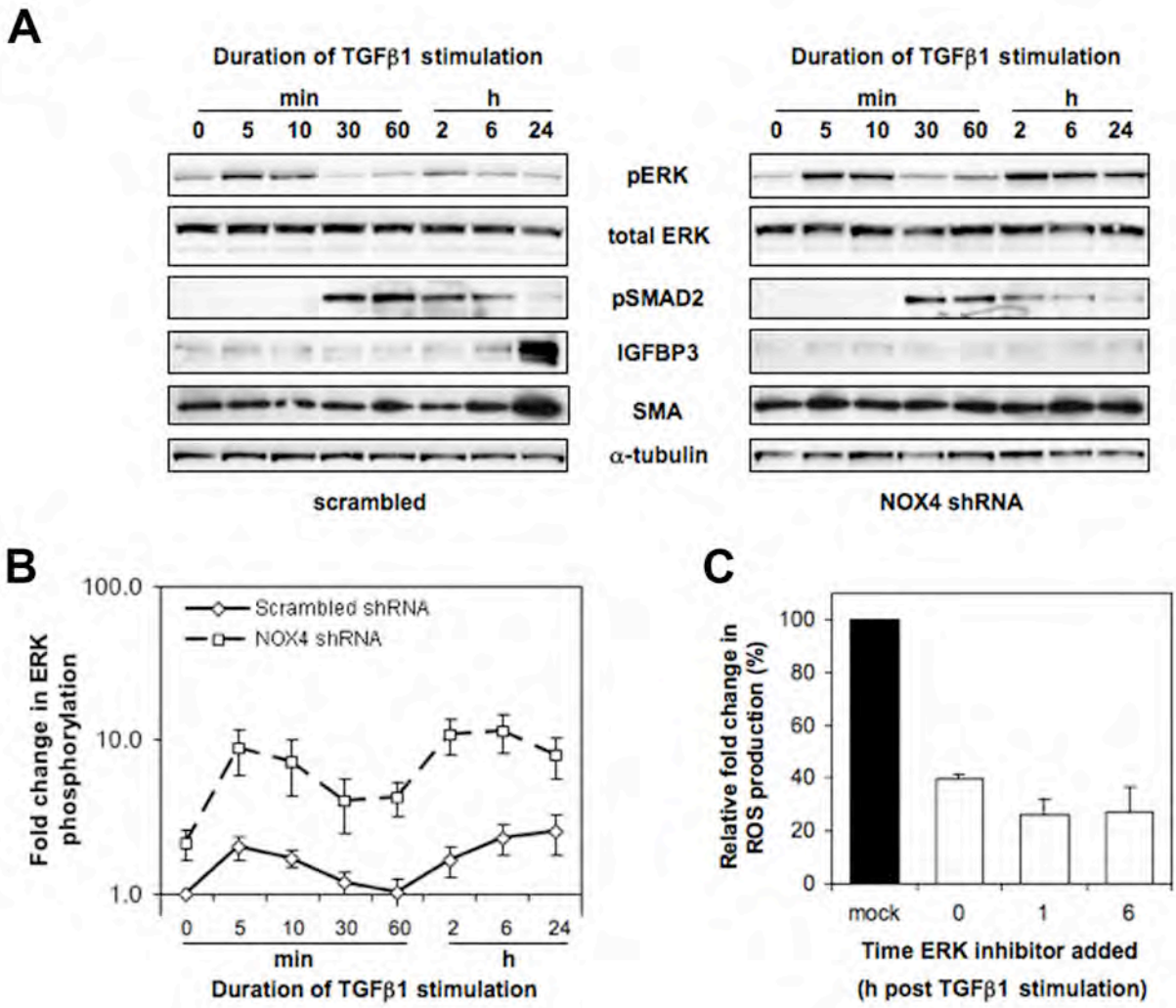

Figure 4

Co-dependency of NOX4-derived ROS production and ERK phosphorylation.

(A) Western blotting with the antibodies indicated of total cell lysates from PrSCs treated with NOX4 or scrambled shRNAs and subsequently stimulated with TGFβ1 for the indicated duration. A representative example of three independent experiments using different donors is shown. (B) Densitometric analysis of phosphorylated ERK in PrSCs treated as in (A). Values represent mean fold change (± SEM) relative to scrambled treated cells at time 0 and normalized against α-tubulin. Three independent experiments using different donors were performed. (C) PrSCs were treated at the indicated time post TGFβ1 stimulation with 50 μM MEK/ERK inhibitor PD98059 or mock and ROS production measured 8 h after TGFβ1 stimulation. Values represent mean fold change in ROS production as percentage (± SEM) relative to mock control treated with TGFβ1 and DMSO equivalent (black bar). Four independent experiments using different donors were performed.

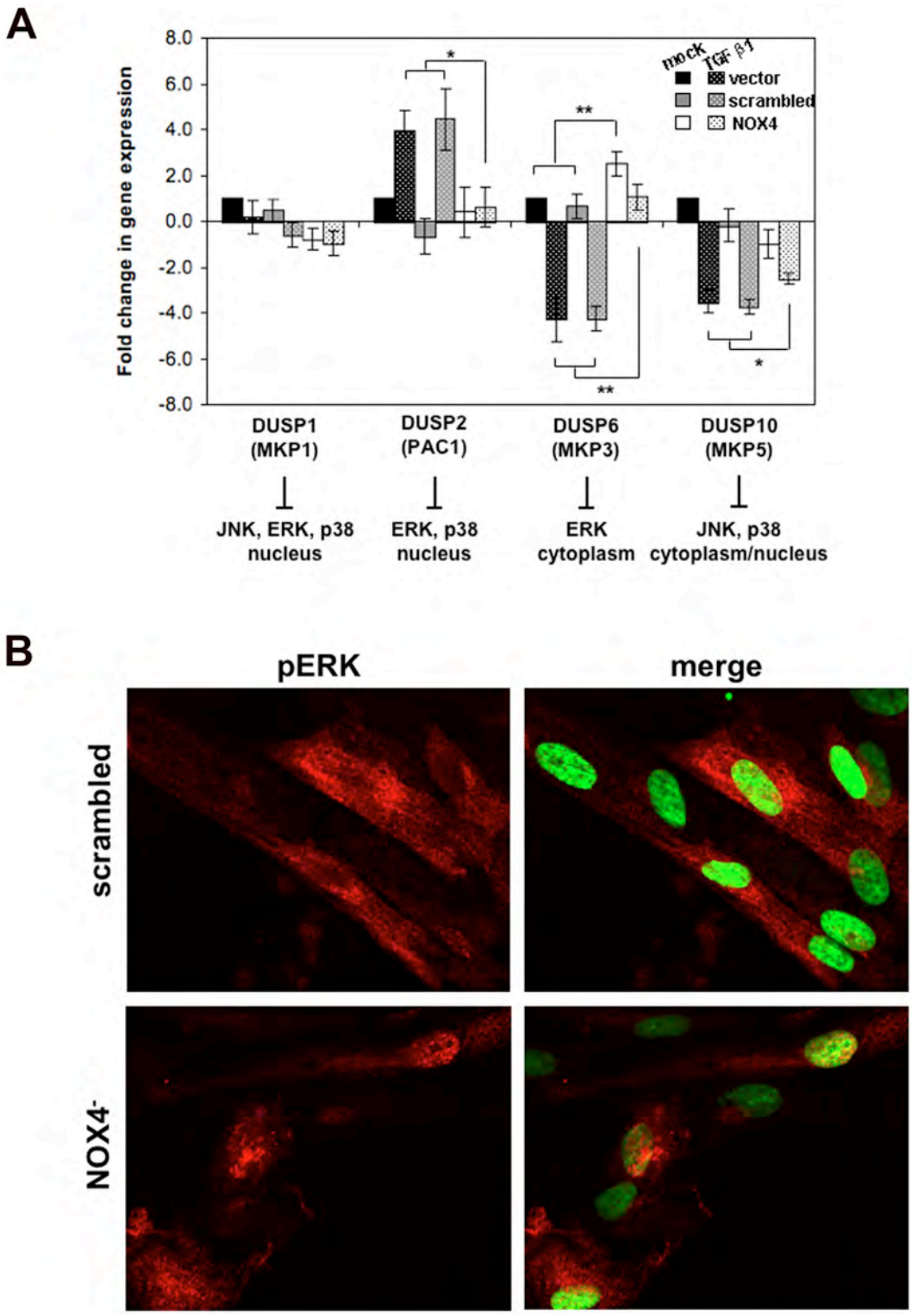

Figure 5
NOX4 coordinates the spatial localization of pERK during transdifferentiation.
(A) qPCR of *DUSP* isoforms in PrSCs treated as Figure 2b at MOI 2.0. Mean fold change in gene expression (± SEM) from four independent experiments using different donors is shown. Significance is indicated (* $p < 0.05$, ** $p < 0.01$). MAPK substrate specificity and subcellular localization of each phosphatase is indicated. (B) PrSCs treated with scrambled or NOX4 shRNAs as in (A) were stimulated with TGFβ1 for 24 h before immunofluorescent staining of pERK (red, left panel). The same image, merged with SYTOX® green nuclear counterstaining is shown (right panel). Magnification x40**.** Images are representative of three independent experiments using different donors.

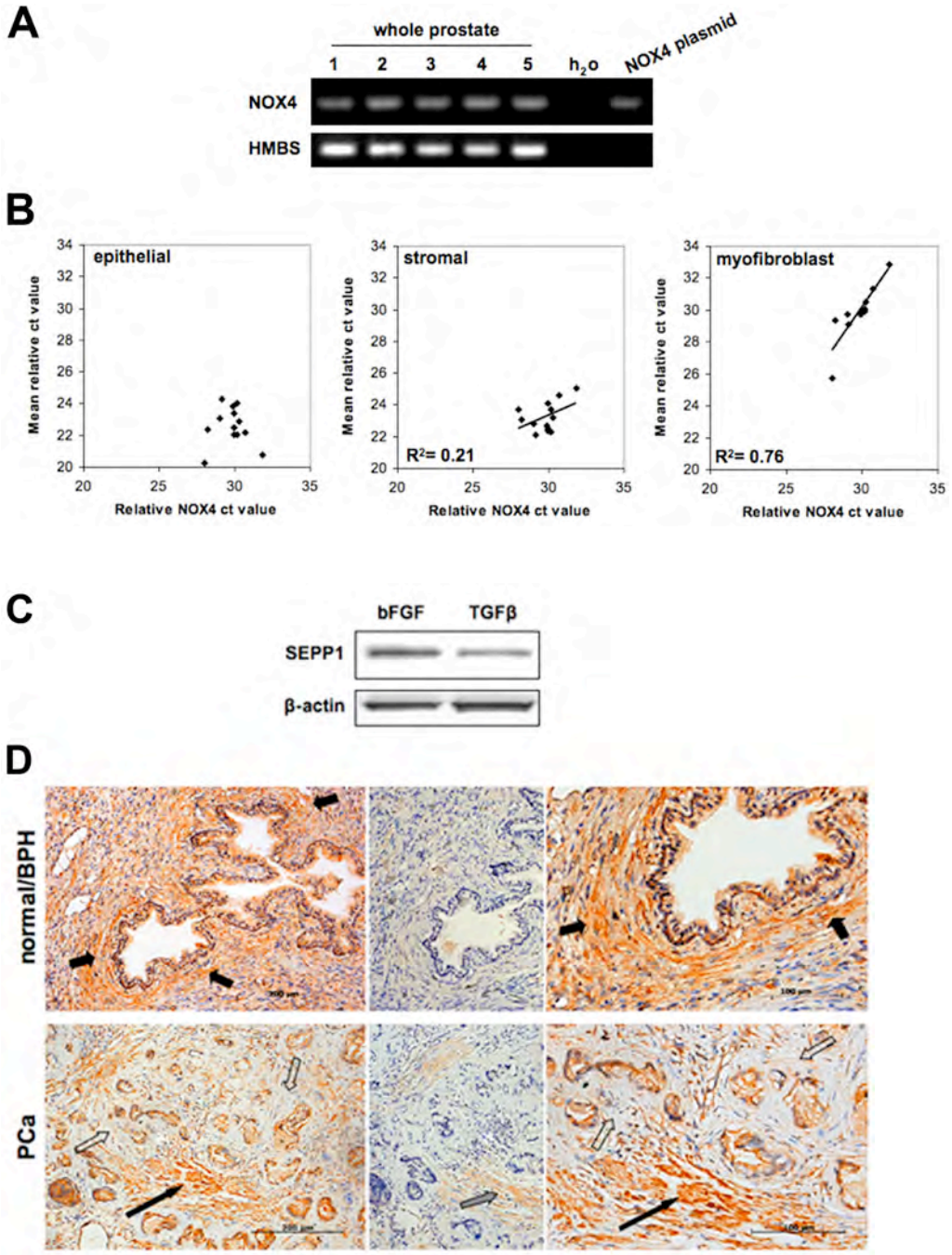

Figure 6

NOX4 and SEPP1 are associated with stromal remodeling *in vivo*. (A, B) *NOX4* expression was evaluated in non-tumor containing human prostate samples. (A) RTPCR of *NOX4* (negative control using water as substrate; positive control using plasmid DNA containing full-length NOX4 cDNA). RTPCR of *HMBS* is shown as loading control. (B) qPCR of *NOX4* in prostate specimens (n =13) relative to the expression of epithelial, stroma or myofibroblast markers as described in Methods. (C) Western blotting of SEPP1 in lysates of PrSCs treated with 1 ng/ml bFGF or TGFβ1 for 24 h. β-actin is shown as loading control. A representative blot of three independent experiments is shown. (D) SEPP1 immunohistochemistry (left) in normal/BPH and PCa biopsies (Gleason 7), enlarged images are shown (right), pre-incubation of anti-SEPP1 antibody with blocking peptide (center). Periglandular stromal cells (short black arrows), periglandular tumor stroma (open arrows), SMC bundles (long black arrow), weak immunostaining of SMCs due to incomplete blocking (grey arrow). Sections were counterstained with Mayer's hematoxylin. Tissue specimens were processed in parallel. Images are representative of two independent experiments with specimens from at least three different donors.

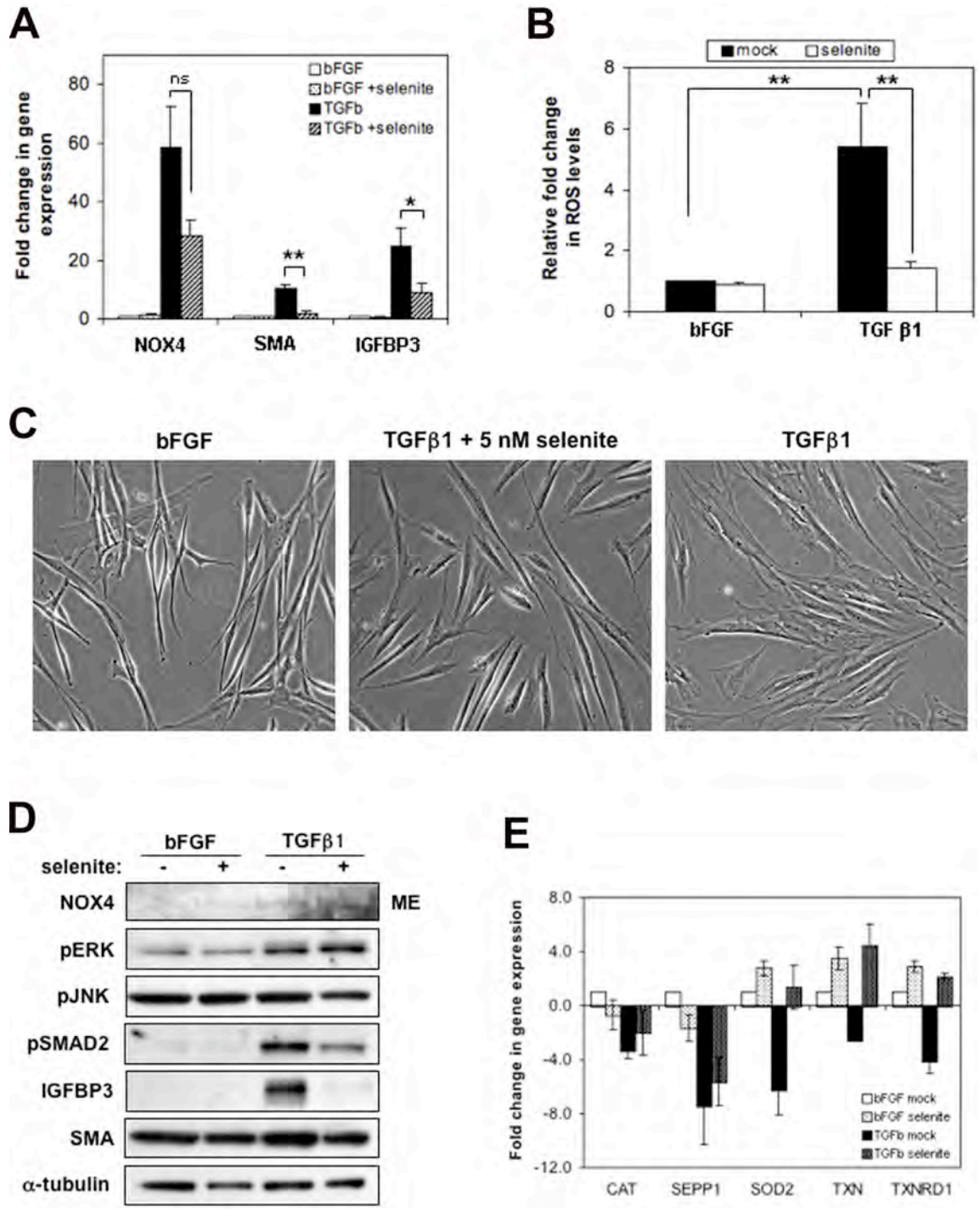

Figure 7

Selenite inhibits TGFβ1-mediated fibroblast-to-myofibroblast transdifferentiation.

PrSCs were pre-treated for 12 h with 5 nM sodium selenite or mock control before stimulation with 1 ng/ml bFGF or TGFβ1 for a further 24 h. Cells were subsequently processed for qPCR of the indicated genes (A, E), ROS determination (B), phase contrast microscopy (C) or Western blotting of total cell lysates using the antibodies indicated (D). For NOX4 detection membrane extract (ME) of cells was prepared in parallel. (C) Magnification x40. Note the thin, elongated and light refractive phenotype of bFGF-treated PrSCs (fibroblasts) in comparison to the flattened and less light refractive morphology of TGFβ1-transdifferentiated PrSCs (myofibroblasts). (C, D) Images are representative of at least four independent experiments using different donors. (A, B, E) Values represent mean fold change (± SEM) relative to bFGF control (without selenite) from four independent experiments using different donors. Significance is indicated (** $p < 0.01$, * $p < 0.05$, ns not significant).

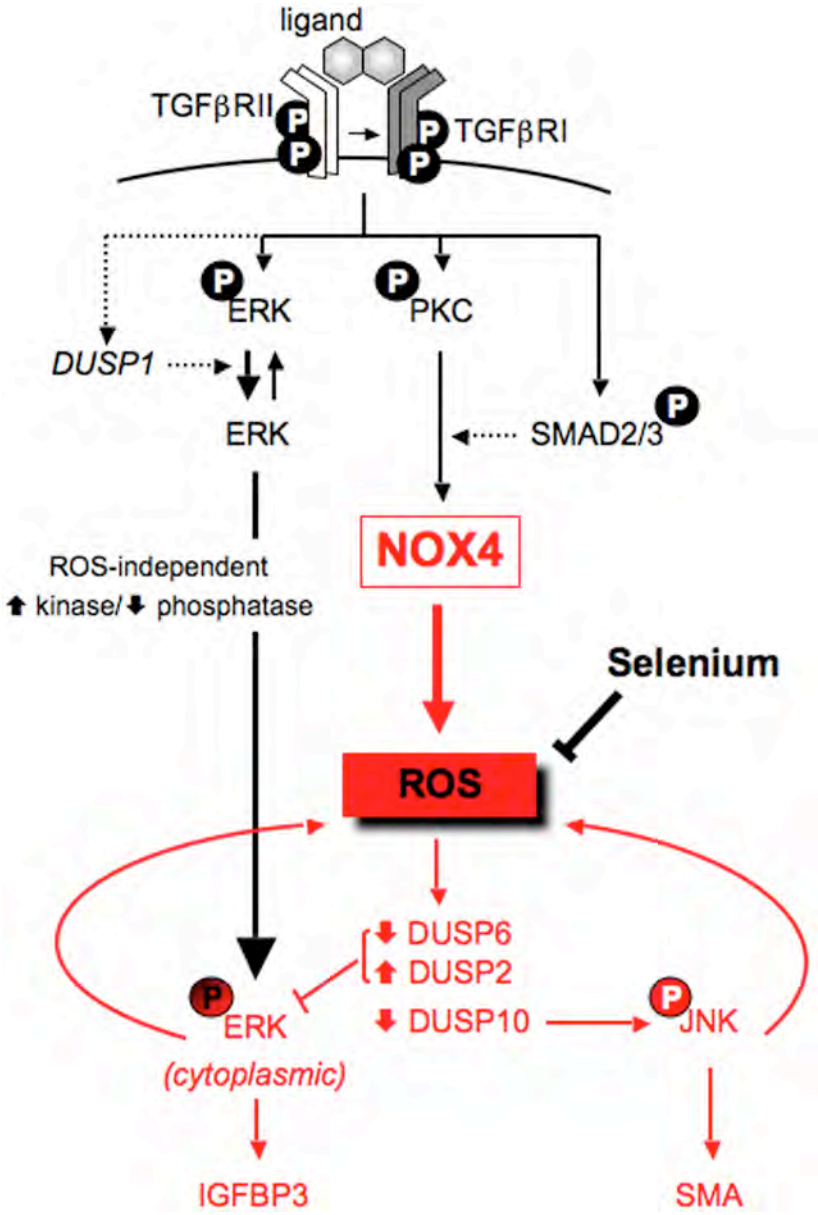

Figure 8
Signaling by NOX4-derived ROS drives TGFβ1-mediated fibroblast-to-myofibroblast transdifferentiation.
Dimeric ligand binding brings homodimers of TGFβRI and TGFβRII into close proximity enabling phosphorylation of TGFβRI by the constitutively active TGFβRII. Activated heterotetrameric TGFβRs subsequently phosphorylate PKC, ERK and the C-terminal domain of SMAD2/3. Transient ERK dephosphorylation may arise via TGFβ1 induction of the immediate early gene (72). *NOX4* transcriptional induction is mediated via Ca^{2+}-indepdent PKC isoforms and other unidentified factors, most likely pSMAD2/3 (24). NOX4-derived ROS promotes sustained JNK phosphorylation via down-regulation of *DUSP10* leading to transcriptional activation of transdifferentiation programs, e.g. SMA. pJNK positively influences ROS production by NOX4 at a post-translational level. Apoptosis induction due to sustained pJNK may be counteracted by survival pathways, including ERK, whose phospho-levels are determined by the relative activity of NOX4-dependent (inhibitory) and NOX4-independent (stimulatory) mechanisms. Late phase ERK phosphorylation is required for NOX4-derived ROS production, which in turn restricts pERK spatially to the cytoplasm via down-regulation of *DUSP6* and up-regulation of *DUSP2*. This promotes activation of cytoplasmic ERK substrates including cytoskeletal proteins (e.g. paxillin and stathmin), cytosolic kinases and transcription factors that induce myofibroblast markers e.g. IGFBP3. (encircled P, phospho-groups: broken arrows, mechanisms presumed to occur during PrSC transdifferentiation but which have been reported by others: black features, NOX4-independent mechanisms; red features, NOX4-dependent mechanisms).

References

1. Sampson, N., Untergasser, G., Plas, E., and Berger, P. 2007. The ageing male reproductive tract. *J Pathol* 211:206-218.

2. Fitzpatrick, J.M. 2006. The natural history of benign prostatic hyperplasia. *BJU Int* 97 Suppl 2:3-6; discussion 21-22.

3. Jacobsen, S.J., Girman, C.J., and Lieber, M.M. 2001. Natural history of benign prostatic hyperplasia. *Urology* 58:5-16; discussion 16.

4. Madersbacher, S., Alivizatos, G., Nordling, J., Sanz, C.R., Emberton, M., and de la Rosette, J.J. 2004. EAU 2004 guidelines on assessment, therapy and follow-up of men with lower urinary tract symptoms suggestive of benign prostatic obstruction (BPH guidelines). *Eur Urol* 46:547-554.

5. Roehrborn, C.G. 2008. BPH progression: concept and key learning from MTOPS, ALTESS, COMBAT, and ALF-ONE. *BJU Int* 101 Suppl 3:17-21.

6. Maddams, J., Brewster, D., Gavin, A., Steward, J., Elliott, J., Utley, M., and Moller, H. 2009. Cancer prevalence in the United Kingdom: estimates for 2008. *Br J Cancer* 101:541-547.

7. Olumi, A.F., Grossfeld, G.D., Hayward, S.W., Carroll, P.R., Tlsty, T.D., and Cunha, G.R. 1999. Carcinoma-associated fibroblasts direct tumor progression of initiated human prostatic epithelium. *Cancer Res* 59:5002-5011.

8. Barclay, W.W., Woodruff, R.D., Hall, M.C., and Cramer, S.D. 2005. A system for studying epithelial-stromal interactions reveals distinct inductive abilities of stromal

cells from benign prostatic hyperplasia and prostate cancer. *Endocrinology* 146:13-18.

9. #Verona, E.V., Elkahloun, A.G., Yang, J., Bandyopadhyay, A., Yeh, I.T., and Sun, L.Z. 2007. Transforming growth factor-beta signaling in prostate stromal cells supports prostate carcinoma growth by up-regulating stromal genes related to tissue remodeling. *Cancer Res* 67:5737-5746.

10. Tiwari, A. 2007. Advances in the development of hormonal modulators for the treatment of benign prostatic hyperplasia. *Expert Opin Investig Drugs* 16:1425-1439.

11. Taplin, M.E. 2008. Androgen receptor: role and novel therapeutic prospects in prostate cancer. *Expert Rev Anticancer Ther* 8:1495-1508.

12. Kyprianou, N., Tu, H., and Jacobs, S.C. 1996. Apoptotic versus proliferative activities in human benign prostatic hyperplasia. *Hum Pathol* 27:668-675.

13. Cardillo, M.R., Petrangeli, E., Perracchio, L., Salvatori, L., Ravenna, L., and Di Silverio, F. 2000. Transforming growth factor-beta expression in prostate neoplasia. *Anal Quant Cytol Histol* 22:1-10.

14. Li, Z., Habuchi, T., Tsuchiya, N., Mitsumori, K., Wang, L., Ohyama, C., Sato, K., Kamoto, T., Ogawa, O., and Kato, T. 2004. Increased risk of prostate cancer and benign prostatic hyperplasia associated with transforming growth factor-beta 1 gene polymorphism at codon10. *Carcinogenesis* 25:237-240.

15. Wikstrom, P., Stattin, P., Franck-Lissbrant, I., Damber, J.E., and Bergh, A. 1998. Transforming growth factor beta1 is associated with angiogenesis, metastasis, and poor clinical outcome in prostate cancer. *Prostate* 37:19-29.

16. Untergasser, G., Gander, R., Lilg, C., Lepperdinger, G., Plas, E., and Berger, P. 2005. Profiling molecular targets of TGF-beta1 in prostate fibroblast-to-myofibroblast transdifferentiation. *Mech Ageing Dev* 126:59-69.

17. Tuxhorn, J.A., Ayala, G.E., Smith, M.J., Smith, V.C., Dang, T.D., and Rowley, D.R. 2002. Reactive stroma in human prostate cancer: induction of myofibroblast phenotype and extracellular matrix remodeling. *Clin Cancer Res* 8:2912-2923.

18. Roberts, A.B., Sporn, M.B., Assoian, R.K., Smith, J.M., Roche, N.S., Wakefield, L.M., Heine, U.I., Liotta, L.A., Falanga, V., Kehrl, J.H., et al. 1986. Transforming growth factor type beta: rapid induction of fibrosis and angiogenesis in vivo and stimulation of collagen formation in vitro. *Proc Natl Acad Sci U S A* 83:4167-4171.

19. Valko, M., Leibfritz, D., Moncol, J., Cronin, M.T., Mazur, M., and Telser, J. 2007. Free radicals and antioxidants in normal physiological functions and human disease. *Int J Biochem Cell Biol* 39:44-84.

20. Trachootham, D., Lu, W., Ogasawara, M.A., Nilsa, R.D., and Huang, P. 2008. Redox regulation of cell survival. *Antioxid Redox Signal* 10:1343-1374.

21. Bedard, K., and Krause, K.H. 2007. The NOX family of ROS-generating NADPH oxidases: physiology and pathophysiology. *Physiol Rev* 87:245-313.

22. Torres, M., and Forman, H.J. 2003. Redox signaling and the MAP kinase pathways. *Biofactors* 17:287-296.

23. Cucoranu, I., Clempus, R., Dikalova, A., Phelan, P.J., Ariyan, S., Dikalov, S., and Sorescu, D. 2005. NAD(P)H oxidase 4 mediates transforming growth factor-beta1-induced differentiation of cardiac fibroblasts into myofibroblasts. *Circ Res* 97:900-907.

24. Hecker, L., Vittal, R., Jones, T., Jagirdar, R., Luckhardt, T.R., Horowitz, J.C., Pennathur, S., Martinez, F.J., and Thannickal, V.J. 2009. NADPH oxidase-4 mediates myofibroblast activation and fibrogenic responses to lung injury. *Nat Med*.

25. Serrander, L., Cartier, L., Bedard, K., Banfi, B., Lardy, B., Plastre, O., Sienkiewicz, A., Forro, L., Schlegel, W., and Krause, K.H. 2007. NOX4 activity is determined by mRNA levels and reveals a unique pattern of ROS generation. *Biochem J* 406:105-114.

26. Block, K., Gorin, Y., and Abboud, H.E. 2009. Subcellular localization of Nox4 and regulation in diabetes. *Proc Natl Acad Sci U S A* 106:14385-14390.

27. Chen, K., Kirber, M.T., Xiao, H., Yang, Y., and Keaney, J.F., Jr. 2008. Regulation of ROS signal transduction by NADPH oxidase 4 localization. *J Cell Biol* 181:1129-1139.

28. Nair, V.D., Yuen, T., Olanow, C.W., and Sealfon, S.C. 2004. Early single cell bifurcation of pro- and antiapoptotic states during oxidative stress. *J Biol Chem* 279:27494-27501.

29. Lee, S.R., Yang, K.S., Kwon, J., Lee, C., Jeong, W., and Rhee, S.G. 2002. Reversible inactivation of the tumor suppressor PTEN by H2O2. *J Biol Chem* 277:20336-20342.

30. Peshavariya, H., Dusting, G.J., Jiang, F., Halmos, L.R., Sobey, C.G., Drummond, G.R., and Selemidis, S. 2009. NADPH oxidase isoform selective regulation of endothelial cell proliferation and survival. *Naunyn Schmiedebergs Arch Pharmacol* 380:193-204.

31. Shono, T., Yokoyama, N., Uesaka, T., Kuroda, J., Takeya, R., Yamasaki, T., Amano, T., Mizoguchi, M., Suzuki, S.O., Niiro, H., et al. 2008. Enhanced expression of NADPH oxidase Nox4 in human gliomas and its roles in cell proliferation and survival. *Int J Cancer* 123:787-792.

32. Lassegue, B., and Clempus, R.E. 2003. Vascular NAD(P)H oxidases: specific features, expression, and regulation. *Am J Physiol Regul Integr Comp Physiol* 285:R277-297.

33. Owens, D.M., and Keyse, S.M. 2007. Differential regulation of MAP kinase signalling by dual-specificity protein phosphatases. *Oncogene* 26:3203-3213.

34. Kondoh, K., and Nishida, E. 2007. Regulation of MAP kinases by MAP kinase phosphatases. *Biochim Biophys Acta* 1773:1227-1237.

35. Mostert, V., Dreher, I., Kohrle, J., and Abel, J. 1999. Transforming growth factor-beta1 inhibits expression of selenoprotein P in cultured human liver cells. *FEBS Lett* 460:23-26.

36. Steinbrenner, H., Alili, L., Bilgic, E., Sies, H., and Brenneisen, P. 2006. Involvement of selenoprotein P in protection of human astrocytes from oxidative damage. *Free Radic Biol Med* 40:1513-1523.

37. Mostert, V., Lombeck, I., and Abel, J. 1998. A novel method for the purification of selenoprotein P from human plasma. *Arch Biochem Biophys* 357:326-330.

38. Low, S.C., Grundner-Culemann, E., Harney, J.W., and Berry, M.J. 2000. SECIS-SBP2 interactions dictate selenocysteine incorporation efficiency and selenoprotein hierarchy. *Embo J* 19:6882-6890.

39. Crane, M.S., Howie, A.F., Arthur, J.R., Nicol, F., Crosley, L.K., and Beckett, G.J. 2009. Modulation of thioredoxin reductase-2 expression in EAhy926 cells: implications for endothelial selenoprotein hierarchy. *Biochim Biophys Acta* 1790:1191-1197.

40. Sturrock, A., Huecksteadt, T.P., Norman, K., Sanders, K., Murphy, T.M., Chitano, P., Wilson, K., Hoidal, J.R., and Kennedy, T.P. 2007. Nox4 mediates TGF-beta1-induced retinoblastoma protein phosphorylation, proliferation, and hypertrophy in human airway smooth muscle cells. *Am J Physiol Lung Cell Mol Physiol* 292:L1543-1555.

41. Seshiah, P.N., Weber, D.S., Rocic, P., Valppu, L., Taniyama, Y., and Griendling, K.K. 2002. Angiotensin II stimulation of NAD(P)H oxidase activity: upstream mediators. *Circ Res* 91:406-413.

42. Hocevar, B.A., Brown, T.L., and Howe, P.H. 1999. TGF-beta induces fibronectin synthesis through a c-Jun N-terminal kinase-dependent, Smad4-independent pathway. *Embo J* 18:1345-1356.

43. Sato, M., Shegogue, D., Hatamochi, A., Yamazaki, S., and Trojanowska, M. 2004. Lysophosphatidic acid inhibits TGF-beta-mediated stimulation of type I collagen mRNA stability via an ERK-dependent pathway in dermal fibroblasts. *Matrix Biol* 23:353-361.

44. Cai, X., Li, M., Vrana, J., and Schaller, M.D. 2006. Glycogen synthase kinase 3- and extracellular signal-regulated kinase-dependent phosphorylation of paxillin regulates cytoskeletal rearrangement. *Mol Cell Biol* 26:2857-2868.

45. Peshavariya, H., Jiang, F., Taylor, C.J., Selemidis, S., Chang, C.W., and Dusting, G. 2009. Translation-linked mRNA destabilization accompanying serum-induced Nox4 expression in human endothelial cells. *Antioxid Redox Signal*.

46. Lyle, A.N., Deshpande, N.N., Taniyama, Y., Seidel-Rogol, B., Pounkova, L., Du, P., Papaharalambus, C., Lassegue, B., and Griendling, K.K. 2009. Poldip2, a novel regulator of nox4 and cytoskeletal integrity in vascular smooth muscle cells. *Circ Res* 105:249-259.

47. Regier, D.S., Greene, D.G., Sergeant, S., Jesaitis, A.J., and McPhail, L.C. 2000. Phosphorylation of p22phox is mediated by phospholipase D-dependent and -independent mechanisms. Correlation of NADPH oxidase activity and p22phox phosphorylation. *J Biol Chem* 275:28406-28412.

48. Tian, Y.C., Chen, Y.C., Chang, C.T., Hung, C.C., Wu, M.S., Phillips, A., and Yang, C.W. 2007. Epidermal growth factor and transforming growth factor-beta1 enhance HK-2 cell migration through a synergistic increase of matrix metalloproteinase and sustained activation of ERK signaling pathway. *Exp Cell Res* 313:2367-2377.

49. Xia, Z., Dickens, M., Raingeaud, J., Davis, R.J., and Greenberg, M.E. 1995. Opposing effects of ERK and JNK-p38 MAP kinases on apoptosis. *Science* 270:1326-1331.

50. Zhang, M., Fraser, D., and Phillips, A. 2006. ERK, p38, and Smad signaling pathways differentially regulate transforming growth factor-beta1 autoinduction in proximal tubular epithelial cells. *Am J Pathol* 169:1282-1293.

51. Svineng, G., Ravuri, C., Rikardsen, O., Huseby, N.E., and Winberg, J.O. 2008. The role of reactive oxygen species in integrin and matrix metalloproteinase expression and function. *Connect Tissue Res* 49:197-202.

52. Edderkaoui, M., Hong, P., Vaquero, E.C., Lee, J.K., Fischer, L., Friess, H., Buchler, M.W., Lerch, M.M., Pandol, S.J., and Gukovskaya, A.S. 2005. Extracellular matrix stimulates reactive oxygen species production and increases pancreatic cancer cell survival through 5-lipoxygenase and NADPH oxidase. *Am J Physiol Gastrointest Liver Physiol* 289:G1137-1147.

53. Steinbrenner, H., and Sies, H. 2009. Protection against reactive oxygen species by selenoproteins. *Biochim Biophys Acta* 1790:1478-1485.

54. Mostert, V., Dreher, I., Kohrle, J., Wolff, S., and Abel, J. 2001. Modulation of selenoprotein P expression by TGF-beta(1) is mediated by Smad proteins. *Biofactors* 14:135-142.

55. Kibriya, M.G., Jasmine, F., Argos, M., Verret, W.J., Rakibuz-Zaman, M., Ahmed, A., Parvez, F., and Ahsan, H. 2007. Changes in gene expression profiles in response to selenium supplementation among individuals with arsenic-induced pre-malignant skin lesions. *Toxicol Lett* 169:162-176.

56. Shilo, S., Pardo, M., Aharoni-Simon, M., Glibter, S., and Tirosh, O. 2008. Selenium supplementation increases liver MnSOD expression: molecular mechanism for hepato-protection. *J Inorg Biochem* 102:110-118.

57. Sarada, S.K., Himadri, P., Ruma, D., Sharma, S.K., Pauline, T., and Mrinalini. 2008. Selenium protects the hypoxia induced apoptosis in neuroblastoma cells through upregulation of Bcl-2. *Brain Res* 1209:29-39.

58. Pence, B.C., Delver, E., and Dunn, D.M. 1994. Effects of dietary selenium on UVB-induced skin carcinogenesis and epidermal antioxidant status. *J Invest Dermatol* 102:759-761.

59. Diwadkar-Navsariwala, V., Prins, G.S., Swanson, S.M., Birch, L.A., Ray, V.H., Hedayat, S., Lantvit, D.L., and Diamond, A.M. 2006. Selenoprotein deficiency accelerates prostate carcinogenesis in a transgenic model. *Proc Natl Acad Sci U S A* 103:8179-8184.

60. Selenius, M., Rundlof, A.K., Olm, E., Fernandes, A.P., and Bjornstedt, M. 2009. Selenium and selenoproteins in the treatment and diagnostics of cancer. *Antioxid Redox Signal*.

61. Li, H., Stampfer, M.J., Giovannucci, E.L., Morris, J.S., Willett, W.C., Gaziano, J.M., and Ma, J. 2004. A prospective study of plasma selenium levels and prostate cancer risk. *J Natl Cancer Inst* 96:696-703.

62. Allen, N.E., Appleby, P.N., Roddam, A.W., Tjonneland, A., Johnsen, N.F., Overvad, K., Boeing, H., Weikert, S., Kaaks, R., Linseisen, J., et al. 2008. Plasma selenium concentration and prostate cancer risk: results from the European Prospective Investigation into Cancer and Nutrition (EPIC). *Am J Clin Nutr* 88:1567-1575.

63. Lippman, S.M., Klein, E.A., Goodman, P.J., Lucia, M.S., Thompson, I.M., Ford, L.G., Parnes, H.L., Minasian, L.M., Gaziano, J.M., Hartline, J.A., et al. 2009. Effect of selenium and vitamin E on risk of prostate cancer and other cancers: the Selenium and Vitamin E Cancer Prevention Trial (SELECT). *Jama* 301:39-51.

64. Duffield-Lillico, A.J., Dalkin, B.L., Reid, M.E., Turnbull, B.W., Slate, E.H., Jacobs, E.T., Marshall, J.R., and Clark, L.C. 2003. Selenium supplementation, baseline

plasma selenium status and incidence of prostate cancer: an analysis of the complete treatment period of the Nutritional Prevention of Cancer Trial. *BJU Int* 91:608-612.

65. Rayman, M.P. 2009. Selenoproteins and human health: Insights from epidemiological data. *Biochim Biophys Acta*.

66. Zhuo, P., and Diamond, A.M. 2009. Molecular mechanisms by which selenoproteins affect cancer risk and progression. *Biochim Biophys Acta* 1790:1546-1554.

67. Pfaffl, M.W. 2001. A new mathematical model for relative quantification in real-time RT-PCR. *Nucleic Acids Res* 29:e45.

68. Rainer, J., Sanchez-Cabo, F., Stocker, G., Sturn, A., and Trajanoski, Z. 2006. CARMAweb: comprehensive R- and bioconductor-based web service for microarray data analysis. *Nucleic Acids Res* 34:W498-503.

69. Wu, Z., Irizarry, R., Gentlemen, R., Martinez-Murillo, F., and Spencer, F. 2004. A model-based background adjustment for oligonucleotide expression arrays. *Journal of the American Statistical Association* 99:909917.

70. Lener, B., Koziel, R., Pircher, H., Hutter, E., Greussing, R., Herndler-Brandstetter, D., Hermann, M., Unterluggauer, H., and Jansen-Durr, P. 2009. The Nadph Oxidase Nox4 Restricts the Replicative Lifespan of Human Endothelial Cells. *Biochem J*.

71. Zenzmaier, C., Untergasser, G., Hermann, M., Dirnhofer, S., Sampson, N., and Berger, P. 2008. Dysregulation of Dkk-3 expression in benign and malignant prostatic tissue. *Prostate* 68:540-547.

72. Schroder, K., Wandzioch, K., Helmcke, I., and Brandes, R.P. 2009. Nox4 acts as a switch between differentiation and proliferation in preadipocytes. *Arterioscler Thromb Vasc Biol* 29:239-245.